Molecular Cloning and Functional Characterization of Psoralen Synthase, the First Committed Monooxygenase of Furanocoumarin Biosynthesis

Romain Larbat, Sandra Kellner, Silvia Specker, Alain Hehn, Eric Gontier, Joachim Hans, Frédéric Bourgaud, Ulrich Matern

THE JOURNAL OF BIOLOGICAL CHEMISTRY VOL. 282, NO. 1, pp. 542–554, January 5, 2007

Molecular Cloning and Functional Characterization of Psoralen Synthase, the First Committed Monooxygenase of Furanocoumarin Biosynthesis*

Received for publication, May 18, 2006, and in revised form, October 25, 2006 Published, JBC Papers in Press, October 26, 2006, DOI 10.1074/jbc.M604762200

Romain Larbat[‡1], Sandra Kellner[§1], Silvia Specker[§], Alain Hehn[‡], Eric Gontier[‡], Joachim Hans[§], Frederic Bourgaud[‡], and Ulrich Matern[§2]

From the [§]Institut für Pharmazeutische Biologie, Philipps-Universität Marburg, Deutschhausstrasse 17A, 35037 Marburg, Germany and the [‡]UMR 1121 Agronomie Environnement INPL-INRA, ENSAIA, 2, av. de la Forêt de Haye, 54505 Vandoeuvre-lès-Nancy, France

***Ammi majus* L. accumulates linear furanocoumarins by cytochrome P450 (CYP)-dependent conversion of 6-prenylumbelliferone via (+)-marmesin to psoralen. Relevant activities, *i.e.* psoralen synthase, are induced rapidly from negligible background levels upon elicitation of *A. majus* cultures with transient maxima at 9–10 h and were recovered in labile microsomes. Expressed sequence tags were cloned from elicited *Ammi* cells by a nested DD-RT-PCR strategy with CYP-specific primers, and full-size cDNAs were generated from those fragments correlated in abundance with the induction profile of furanocoumarin-specific activities. One of these cDNAs representing a transcript of maximal abundance at 4 h of elicitation was assigned CYP71AJ1. Functional expression in *Escherichia coli* or yeast cells initially failed but was accomplished eventually in yeast cells after swapping the N-terminal membrane anchor domain with that of CYP73A1. The recombinant enzyme was identified as psoralen synthase with narrow substrate specificity for (+)-marmesin. Psoralen synthase catalyzes a unique carbon-chain cleavage reaction concomitantly releasing acetone by *syn*-elimination. Related plants, *i.e. Heracleum mantegazzianum*, are known to produce both linear and angular furanocoumarins by analogous conversion of 8-prenylumbelliferone via (+)-columbianetin to angelicin, and it was suggested that angelicin synthase has evolved from psoralen synthase. However, (+)-columbianetin failed as substrate but competitively inhibited psoralen synthase activity. Analogy modeling and docked solutions defined the conditions for high affinity substrate binding and predicted the minimal requirements to accommodate (+)-columbianetin in the active site cavity. The studies suggested that several point mutations are necessary to pave the road toward angelicin synthase evolution.**

Furanocoumarins are produced by many plants, mostly of the Apiaceae, Rutaceae, Moraceae, or the *Coronilla* and *Psoralea* genera of the Fabaceae (1–3). Multiple pharmacological effects have been ascribed to several of these metabolites (4–6), which were included in clinical screenings but received attention also for their inhibitory effect on monooxygenases involved in drug metabolism (7–9) and potential toxicity (10). The (dihydro)furan-substituted *2H*-1-benzopyran-2-one forms the characteristic core structure, and the annulation type distinguishes the linear furanocoumarins or psoralens from the angular furanocoumarins (Fig. 1). It is noteworthy that plants accumulate either psoralens only, *e. g. Ammi majus* (11–13), *Petroselinum crispum* (14, 15), and *Coronilla* sp (16), or both types of compounds, whereas the exclusive production of angular furanocoumarins has never been reported (1). Furanocoumarins often accumulate in the surface wax of tissues and can easily be collected in washes with organic solvents (17, 18). Such surface coating was considered to protect the plants from fungal invasion or herbivore attack (19), because potent antimycotic activity has been documented for furanocoumarins *in vitro* (20), and the few insects utilizing furanocoumarin-producing plants as an ecological niche, *i.e.* the black swallowtail butterfly, depend on a particular detoxifying machinery (21). The toxicity to insects is conceivably a consequence of both DNA modification and monooxygenase inhibition. Furanocoumarins intercalate in double-stranded DNA, and psoralens are known to cross-link pyrimidine bases under irradiation by [2 + 2]cycloaddition via their 3,4- and 2′,3′-double bonds, whereas angular furanocoumarins form only monoadducts for steric reasons (22). Although the angular compounds are not as potent antifeedants as the psoralens (23), the combination of angular and linear furanocoumarins shows synergistic effects (24, 25) presumably because the angular compounds inhibit monooxygenases required for the detoxification of psoralens (26, 27). This fact and the relatively limited distribution of angular furanocoumarins suggested that the supplementary production of angular furanocoumarins has evolved as a sophisticated means of plants to counter the detoxification mechanisms of herbivores (28–30). It is conceivable that this capability has developed as a modification of the pathway to linear furanocoumarins at a late stage in the evolution.

The flow of carbon in furanocoumarin biosynthesis is known since decades from precursor feeding studies (1) and proceeds from 4-coumaric acid via umbelliferone, which is prenylated in either the 6- or 8-position to give demethylsuberosin and osthenol, respectively (Fig. 1). Whereas the subcellular compartment and the precise mode of cyclization of 4-coumaric acid to

* This work was supported in part by the Ministère de la Recherche et de l'Enseignement Supérieur (to F. B.) and by the Deutsche Forschungsgemeinschaft and Fonds der Chemischen Industrie (to U. M.). The costs of publication of this article were defrayed in part by the payment of page charges. This article must therefore be hereby marked "*advertisement*" in accordance with 18 U.S.C. Section 1734 solely to indicate this fact.

[1] These authors contributed equally to the work presented.

[2] To whom correspondence should be addressed. Tel.: 49-64212822461; Fax: 49-64212826678; E-mail: matern@staff.uni-marburg.de.

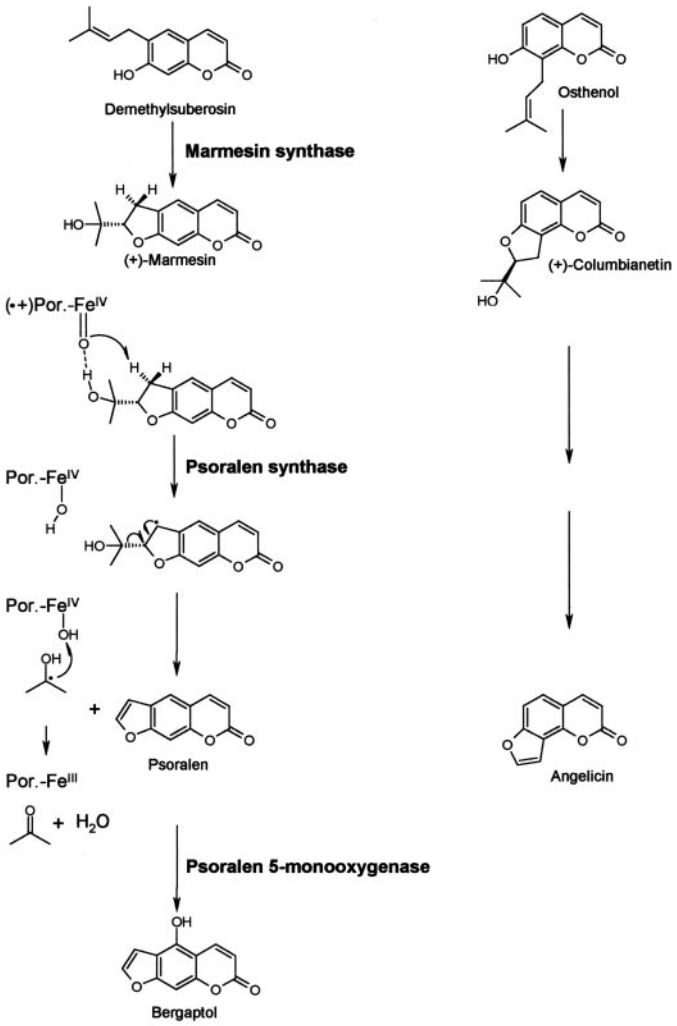

FIGURE 1. **Pivotal cytochrome P450-dependent reactions in the linear furanocoumarin pathway converting 6-prenylumbelliferone (demethylsuberosin) via (+)-marmesin to psoralen and bergaptol or xanthotoxol.** The analogous pathway to angular furanocoumarins is shown for comparison, but has not been established *in vitro*. The ferryl(IV)-enzyme is likely the oxidizing species, because the one-step elimination of acetone excludes a nucleophilic enzyme-peroxide complex for catalysis.

umbelliferone have remained elusive (31), the 6-prenyltransferase was assigned to plastids in *Ruta graveolens* (32), which is compatible with the mevalonate-independent prenylation of umbelliferone observed in *Apium graveolens* (33). An equivalent location is likely for the 8-prenyltransferase activity, although this has not been as firmly documented. All subsequent steps converting demethylsuberosin to psoralen or osthenol to angelicin are supposedly catalyzed by highly analogous enzymes (34), but only the linear series has been studied in detail. Enzyme studies conducted mostly with elicited *A. majus* or *P. crispum* cells (35–38) identified marmesin and psoralen synthases as well as psoralen 5-monooxygenase as separate cytochrome P450 (CYP)[3] entities for the consecutive conversion of demethylsuberosin to bergaptol, which then is methylated to bergapten (39). These studies became possible, because furanocoumarins are completely lacking from the cell suspensions propagated in the dark but accumulate rapidly in the cells and culture fluid upon treatment with fungal elicitor. Nevertheless, the specific CYP activities of crude microsomes were rather low, on average, and varied greatly with the plant type and growth stage of cells. Significant conversion rates were accomplished with microsomes from *A. majus* cells propagated in suspension no longer than 5 months and treated for 5–10 h with elicitor. Moreover, the CYP activities of isolated microsomes turned out rather labile even on storage at −70 °C, which ruled out any purification. Overall, the time course of furanocoumarin accumulation and the induction of CYP activities suggested a window of about 2–6 h of elicitation for maximal abundance of the committed transcripts.

Marmesin synthase, psoralen synthase, and psoralen 5-monooxygenase catalyze very different reactions with psoralen synthase (Fig. 1) catching most the attention. Although oxidative carbon-chain cleavage reactions are common in nature, such as in homoterpene (40) or steroid biosynthesis (41), the true mechanism has remained under debate (41). The psoralen synthase activity of *A. majus* microsomes was examined with position and stereospecifically deuterated marmesin substrates (42) and revealed the unique release of acetone as byproduct. The reaction probably initiates at C-3′ (Fig. 1), and it is noteworthy that psoralen synthase, in contrast to chemical model reactions (43), abstracts the hydrogen *syn*-configurated to the shielding isopropyloxy group (Fig. 1). This is a consequence of the radical mode of the reaction requiring that all partners be confined to a cage (43). The same kind of mechanism appears to operate in the pathway to angular furanocoumarin in *Heracleum mantegazzianum*, where the conversion of (+)-columbianetin to angelicin (Fig. 1) proceeds by *syn*-elimination (34). These data further supported the assumption that the angular pathway has evolved from psoralen biosynthesis, although the release of acetone has not been confirmed for *Heracleum*, and final proof must await the alignment of enzyme sequences.

In contrast to the basic course of biosynthesis, the molecular genetics of furanocoumarin formation has remained largely unresolved due, in part at least, to the lability of the consecutively operating P450s. As an initial step, we describe here the cloning and functional expression of the psoralen synthase from *A. majus*, the first furanocoumarin-committed monooxygenase gene. The recombinant enzyme revealed narrow specificity for (+)-marmesin, whereas (+)-columbianetin, which is considered as the analogous precursor of the angular furanocoumarin angelicin acted as a competitive inhibitor only. Nevertheless, supplemental insight from molecular modeling and docking approaches seemed to support the idea that psoralen synthase may have evolved also angelicin synthase activity through a limited number of point mutations fitting the active site to the metabolism of (+)-columbianetin.

EXPERIMENTAL PROCEDURES

Chemicals—Umbelliferone, psoralen, xanthotoxin, (+)-pulegone, and cinnamic acids were purchased from Sigma-Aldrich, and xanthotoxol, menthofuran or HPLC-grade 4-cou-

[3] The abbreviations used are: CYP, cytochrome P450; SRS, substrate recognition site; C4H, cinnamate 4-hydroxylase; MOPS, 4-morpholinepropanesulfonic acid; ORF, open reading frame; nt, nucleotide; RACE, rapid amplification of cDNA ends; UTR, untranslated region; PBD, Protein Data Bank.

maric acid were from Roth (Karlsruhe, Germany) and Fluka (Buchs, Switzerland), respectively. Angelicin, bergapten, and bergaptol were purchased from Extrasynthese (Genay, France). Isoproturon and chlortoluron were from CIL (Paris, France). Demethylsuberosin was synthesized as described previously (36), and (+)-marmesin, 5-hydroxymarmesin, and (+)-3,4,2′,3′-D_4-columbianetin were kindly provided by G. Innocenti (Faculty of Pharmacy, Padova, Italy) and W. Boland (Max-Planck Institut für Chemische Ökologie, Jena, Germany). Hybond-N^+ filters and Rediprime™ II Random Prime Labeling kit were from Amersham Biosciences and [α-^{32}P]dCTP was bought from MP Biomedicals. TaqDNA polymerase, MMLV-reverse transcriptase, restriction endonucleases XhoI, PvuII, BamHI, and PaeI or AccSure DNA polymerase were purchased from MBI Fermentas (St. Leon-Rot, Germany) and Bioline (Luckenwalde, Germany), respectively.

Cell Cultures and Separation of Coumarins—Cell suspensions of *A. majus* L. (40-ml B5 cultures in 250-ml flasks) were propagated continuously in the dark at 21–24 °C, and 7-day-old cultures were treated with crude *Phytophthora sojae* cell wall elicitor (5 mg/40 ml, sterilized in 1 ml of water) as described earlier (35, 36). Control cultures received sterile distilled water only. The cells were harvested by vacuum filtration at various time intervals up to 32 h, washed twice with sterile distilled water, frozen in liquid nitrogen, and stored at −70 °C until use. The culture fluid and wash were combined, and coumarins were separated by HPLC in a solvent system described elsewhere (44) employing a nucleosil C-18 column (5 μm, 4 × 12.5 cm) and a step gradient from 1.5% *ortho*-phosphoric acid (A) and 80% aqueous acetonitrile (B) starting at 90% A in B, decreasing to 50% A in B over 20 min, and followed by 100% B for an additional 10 min. The elution at 1.0 ml/min was monitored by ultraviolet absorbance (350 nm), and psoralen (*Rt* 20.0 min) was completely separated under these conditions from bergaptol (18.4 min), xanthotoxol (15.6 min), marmesin (16.0 min), demethylsuberosin (26.8 min), umbelliferone (12.0 min), and 4-coumaric acid (11.7 min).

cDNA Cloning—Total RNA was isolated from elicitor-induced (1–6 h) and control cells as published elsewhere (45), and cDNA was synthesized with the anchor primer (AP) CCACGCGTCGACTAGTAC$(dT)_{17}$. First strand cDNA was amplified with Taq polymerase, and cytochrome P450-related ESTs were then generated in separate reactions using AP and one of the four primers derived from the conserved PERF motif (EEF*X*PER; Fig. 2*C*) (46). Each incubation was subsequently diluted 1:1000 and amplified in a second round of nested PCR using eight decamer primers inferred from the PFG motif (Fig. 2*C*) in combination with AP (47). The cDNA fragments were cloned, the full-length clones were generated by RNA ligase-mediated RACE (48), and the products were ligated into pCR® 4-TOPO Vector (Invitrogen) for multiplication in Top10F host (Invitrogen). The cDNA for final sequencing (primer-walking) was amplified by proofreading PCR (0.5 mM primer, 2.0 mM $MgSO_4$, 56 °C annealing temperature) with AccSure DNA polymerase-activated (94 °C for 10 min) prior to 35 cycles of 0.5 min of denaturation, 1.0 min of annealing, and 2.0 min of extension. Purification of the cDNAs before RACE and sequencing was carried out with High Pure PCR Product Purification kit (Roche Diagnostics, Mannheim, Germany). Sequence analysis was achieved with advanced WU-Blast2 (EMBL) and alignments with ClustalW (EMBL-EBI). The induction of specific transcript abundance was monitored by semiquantitative PCR (Fig. 2*B*) using end-to-end primers (forward 5′-GCAGAGTGCAGAGCAATAGAAATGAAGATGC and reverse 5′-GAGCTGGGAATGAGTATTGACATGG). Genomic DNA was isolated by a standard procedure (49) from adult *A. majus* plants freshly harvested from the Botanical Gardens, the *CYP71AJ1* gene was amplified by PCR employing the end-to-end primers, and the gene was ligated into the pCR®4-TOPO Vector (Invitrogen) for sequencing.

Northern and Southern Blotting—Samples of total RNA isolated from the induced cells at various time points of elicitation (up to 32 h) were densitometrically quantified after 1.5% agarose gel electrophoresis, and aliquots (4 μg per time point) were dissolved in (30.0 μl) 0.5 M MOPS buffer, pH 7.0, 50% formamide containing 2.2 M formaldehyde. Following the denaturation at 68 °C for 15 min, the samples were transferred onto Hybond-N^+ filters in a Minifold I device (Schleicher & Schüll, Dassel, Germany). The filters were dried for 2 h at 80 °C and then prehybridized at 68 °C for 3 h with 0.025% salmon sperm DNA in 5× SSC, 2× Denhardt's solution containing 0.1% SDS. Full-length *CYP71AJ1* cDNA was labeled with [α-^{32}P]dCTP using the Rediprime™ II Random Prime Labeling kit, purified through a Sephadex G_{50} column and employed as a probe in Northern blotting. The RNA was hybridized at 68 °C for 16 h, the filter washed subsequently twice at 68 °C with 2× SSC containing 0.1% SDS and twice with 1× SSC containing 0.1% SDS before exposure to an imaging plate. The radioactivity was spotted by a Bioimager FLA 2000 (Fuji Photo Film, Tokyo, Japan).

For Southern blotting, the genomic DNA was isolated from *A. majus* leaf tissue (49), resuspended in sterile distilled water and stored at 4 °C until use. Digestion (20 μg of DNA per incubation) was accomplished overnight with endonucleases XhoI, PvuII, BamHI, or PaeI, and the restriction fragments were separated by gel electrophoresis at 70 V for 4 h on 0.8% agarose containing 0.4 μg/100 ml ethidium bromide. The DNA was depurinated in 0.25 N HCl for about 20 min, denatured with 0.5 N NaOH containing 1.5 M NaCl for 40 min and neutralized twice for 30 min with 0.5 M Tris-HCl, pH 7.4 in the presence of 1.5 M NaCl. The DNA was transferred for 20 h onto a Hybond-N^+ filter in 20× SSC. The membrane was dried, washed (2× SSC), prehybridized (5× SSPE, 5× Denhardt's containing 0.2% SDS), and the cDNA was labeled with [α-^{32}P]dCTP as described above. The hybridized filter was washed at 68 °C successively twice with 2× SSC, twice with 1× SSC, and twice with 0.1× SSC, all in the presence of 0.1% SDS, and exposed to an imaging plate for Bioimager FLA 2000 analysis.

Expression Constructs—The ORF of *CYP71AJ1* was amplified by PCR and introducing KpnI and EcoRI restriction sites proximal upstream to the start ATG and downstream to the stop codon (TGA) employing end-to-end primers (forward 5′-CGGTACCATGAAGATGCTGGAACAGAAT and reverse GGAATTCTCAAACATGTGGTCTGGCAACCACCAAGAGAGG). The incubation was heated to 95 °C for 5.0 min prior to 30 cycles of 30 s

denaturation at 95 °C followed by 45 s of annealing at 50 °C and a 2.0-min extension at 72 °C. The reaction was finished by an additional 10.0-min extension at 72 °C. The product was purified through agarose gel electrophoresis, digested with KpnI and EcoRI, and the fragment of 1490 bp was ligated into yeast expression vector pYEDP60 (50). The identity of the expression plasmid was verified by restriction and sequence analyses prior to the transformation of yeast cells.

Substitution of the N-terminal membrane anchor region (37 amino acids) in *CYP71AJ1* by the corresponding region of *CYP73A1* (33 amino acids) generated the mutant *CYP71AJ1mut*. A primer was designed corresponding to the amino acid sequence Arg^{27}–Leu^{33} of *Cyp73A1* fused to residues Pro^{38}–Pro^{45} of *Cyp71AJ1* (reverse primer 5′-GGGATATTGTGGTGGAGAAGGTGGGAGCTTGAATTTTTTACCGCGG) and employed for PCR with the *CYP73A1* cDNA template in combination with another primer (forward 5′-GGATCCATGGACCTCCTCCTCATAGA) creating a BamHI restriction site upstream of the ATG. This first amplification generated a product of 123 nt composed of the upstream 99 nt of *CYP73A1* followed downstream by 24 nt of *CYP71AJ1*. This product was agarose-purified and used in a second PCR as a sense primer together with the reverse primer 5-CGAATTCAAAGCAACTGCAAGTGAAA and *CYP71AJ1* cDNA as template. In both cases, the PCR mixture was preheated for 5 min at 95 °C, followed by 10 cycles of 30 s denaturation at 95 °C, 45 s annealing at 60 °C during the first cycle and decreasing by 1 °C for each cycle, and a 2.0-min extension at 72 °C. Additional 20 cycles were performed with the annealing temperature maintained at 50 °C, and the PCR was terminated with a final extension of 10 min at 72 °C. The end product *CYP71AJ1mut*, corresponding to a nearly full-size *CYP71AJ1* sequence but harboring a replacement of the upstream 111 nt by the upstream 99 nt of *CYP73A1*, was flanked in 5′ and 3′ by BamHI and EcoRI sites, respectively, which were used for ligation into the pYeDP60 yeast expression vector. The identity of the resulting plasmid was verified by restriction and sequence analyses.

Yeast Expression and Enzyme Assays—Yeast strain WAT11, engineered to overexpress the P450 reductase isoform ATR1 from *Arabidopsis thaliana* upon galactose induction (50), was transformed with the various pYeDP60 expression constructs as described elsewhere (51). Propagation of yeast cells and preparation of microsomes were conducted as described previously (50). Single colonies from SGI plates were transferred into SGI liquid medium (10 ml) and grown at 28 °C for 24 h. An aliquot of the culture (5 ml) was transferred subsequently into YPGE growth medium (200.0 ml), and growth was continued for an additional 24 h at 28 °C. Expression of P450 was then induced by the addition of galactose (20.0 g/liter growth medium). The induction was conducted for 18 h at 20 °C, before the cells were harvested, and the microsomal fraction collected by precipitation in the presence of 0.05 M $MgCl_2$ (52). Protein amounts were determined according to Bradford (53), and the microsomal P450 contents were determined as described by Omura and Sato (54).

CYP71AJ1 Substrate Specificity—Each compound listed in Table 1 was tested as a potential substrate for *CYP71AJ1*. Briefly, microsomes isolated from yeast *CYP71AJ1mut* transformants were incubated in 0.1 M sodium phosphate buffer, pH 7.0 (150.0 μl total), containing 200 μM of potential substrate, in the presence of 1.0 mM NADPH or without NADPH (control). The assay mixture was equilibrated for 2.0 min at 27 °C prior to starting the reaction by the addition of microsomes. After 1 h at 27 °C the reaction was terminated by adding 75.0 μl of acetonitrile/conc. HCl (99:1), and product formation as well as substrate consumption was analyzed by reverse-phase HPLC on a Purospher 5 μm, 4 × 125-mm endcapped column (Merck). The column was equilibrated in water/acetic acid/acetonitrile (98:1:1) at a flow rate of 0.9 ml/min, and the elution was performed under diode array detection (220–400 nm) using a convex gradient of acetonitrile/methanol (1:1) from 0 to 60% for 25.0 min, followed by 100% acetonitrile/methanol (1:1) for an additional 10 min. Bioconversion of (+)-marmesin to psoralen was directly assessed in yeast cultures. Yeast cells transformed with *CYP71AJ1*, *CYP71AJ1mut*, or the empty vector were grown in YPGE medium and induced for P450 expression by the addition of galactose. (+)-Marmesin was added to a final concentration of 1.0 mM, and the cells were incubated for an additional 4 h at 24 °C. The composition of the culture fluid was analyzed subsequently by HPLC at 300 nm, using the separation method described above.

Psoralen Synthase Kinetic Analyses—Kinetic assays were conducted for 6.0 min in 0.1 M sodium phosphate buffer, pH 7.0 (200.0 μl total), containing 1.0 mM NADPH and 0.3 pmol of wild-type or mutant CYP71AJ1, and varying the concentration of (+)-marmesin. Competitive inhibition assays with (+)-3,4,2′,3′-D_4-columbianetin were conducted by adding from 10.0 to 300.0 μM of inhibitor to the reaction medium. The apparent K_m was determined by Lineweaver-Burk extrapolation. Mechanism-based inactivation assays were performed by preincubating the microsomes (1.7 pmol of P450) in 0.1 M sodium phosphate buffer, pH 7.0 (60.0 μl total) at 27 °C with 0.05 mM of either one of the inhibitor compounds in the presence or in the absence of 1.0 mM NADPH, because mechanism-based inhibition depends on NADPH. P450s are furthermore known to undergo partial auto-inactivation in the presence of NADPH. After 10.0 min, aliquots (20.0 μl) of the preincubation were transferred for comparative psoralen synthase assays into the final incubation mix of 0.1 M phosphate buffer, pH 7.0 (200.0-μl total) containing 1.0 mM NADPH and 0.15 mM (+)-marmesin. The reactions were stopped after an additional 10.0 min at 27 °C by addition of acetonitrile/conc. HCl (99:1), and psoralen was quantified by HPLC separation. The residual activity was expressed as the percentage of the activity measured in control incubations carried out with 1.0 mM NADPH in the absence of inhibitor (100% corresponding to 300 min^{-1}). The activity score recorded for psoralen, 5-methoxypsoralen, 8-methoxypsoralen or angelicin after preincubation in the presence of NADPH ranged from 87 ± 3% to 95 ± 2%, while the preincubation in the absence of NADPH reduced the activity to 78 ± 8%, which was negligibly affected by the psoralens or angelicin.

GC-MS Analysis—The product eluting from HPLC at a retention time corresponding to psoralen was collected from 20 incubations, the solvent was evaporated in an air stream, and the pellet was resuspended in trichloromethane for GC-MS

analysis. The sample (1.0 μl) was injected into a Varian Star 3400 CX spectrometer fitted with a Varian factor Four 5MS column (15.0 m × 0.25 mm inner diameter, 0.1-μm film) using helium at 5.5 psi as carrier gas. The column temperature was initially 90 °C for 3 min, ramped to 180 °C at 10 °C × min^{-1}, then to 230 °C at 5 °C × min^{-1}, finally to 250 °C at 10 °C × min^{-1}, and held for 5.0 min. Mass spectra were recorded at 70 eV, scanning from 30 to 400 atomic mass units and compared with authentic psoralen standard.

Site-directed Mutagenesis of CYP71AJ1mut—Site-directed mutagenesis of *CYP71AJ1mut* was carried out using a two-stage PCR procedure. In a first round, two separate fragments were created, corresponding to the 5′- and 3′-end of the clone, both carrying the desired mutation. To introduce the mutation M120V, the 5′-fragment was amplified using the 73A1ntBam forward primer (5′-GGATCCATGGACCTCCTCCTCA-TAGA-3′) with the M120Vrev primer (5′-GTGTAACGAG-CAAACACGACGTCCTTCCCATTGTAGAAG-3′, mutated sites are underlined); the 3′-fragment was obtained by using the M120Vforw primer (5′-CTTCTACAATGGGAAGGACGTC-GTGTTTGCTCGTTACAC) with the 71AJ1Eco reverse primer (5′- GGAATTCTCAAACATGTGGTCTGGCAACC-ACCAAGAGAGG-3′). Both reactions were carried out using *Pfx* DNA polymerase (Invitrogen) with a program consisting of an initial preheating step of 5 min at 94 °C, followed by 5 cycles with 30 s denaturation at 94 °C, 30 s annealing at 30 °C, and 90 s extension at 68 °C. Subsequently, 25 cycles were performed with an annealing temperature of 55 °C. After a final extension phase for 10 min at 68 °C, both amplified fragments were agarose-purified using Qiaquick Gel Extraction kit (Qiagen). To merge the 5′- and 3′-ends of the clone, a second round of PCR (conditions as described above) was carried out using both fragments as templates and primers 73A1ntBam and 71AJ1Eco. The resulting PCR fragment was ligated into the pCR8 vector (Invitrogen). Success of the mutation was verified by sequencing. Finally, subcloning into pYeDP60 was performed by ligating the 1.5 kb of EcoRI/BamHI *Cyp71AJ1mutM120V* fragment into the linearized vector. Expression of the generated mutant was performed as described above for *Cyp71AJ1mut*.

Enzyme Modeling and Docking Studies—The CYP71AJ1 homology model was built using the MOE program (Chemical Computing Group, Montreal, Canada) and according to Baudry *et al.* (55). A multiple sequence alignment between CYP71AJ1 and six crystallized P450s (CYP2C5 (PDB: 1DT6), CYP2C9 (PDB: 1OG2), CYP2C8 (PDB: 1PQ2), CYP2B4 (PDB: 1PO5), CYP2A6 (PDB: 1Z11), and P450 BM3 (PDB: 1BU7)) was done using the Blosum 62 substitution matrix. The sequence alignment was then homology-modeled using the structure of CYP2C8 (27.5% similarity with CYP71AJ1) as template. With the MOE program, 10 models were generated, minimized in a first round to remove poor Van der Waals contacts and ranked according to MOE residue packing quality function. The best model was selected, and the heme coordinates from CYP2C8 were added by creating a covalent bond between the heme iron atom, and the sulfur of the conserved cysteine. The structure was finally minimized using the CHARMm22 force field until the final energy gradient was <0.01 kcal/mol·Å. For the docking simulation, marmesin, and columbianetin were created with the molecular builder application from MOE program and minimized using the CHARMm22 force field. Prior to the docking simulation, an oxygen atom was added to the heme to represent the iron-oxo intermediate. Docking of marmesin and columbianetin was simulated using the Monte Carlo procedure. For each substrate, 25 docking models were created and ranked according to the sum of the substrate internal energy and the Van der Waals and the electrostatic energies. The best ranked model was selected, and the complex substrate/protein was minimized using MMFF94 force field.

Phylogenetic Analysis—Sequences were taken from the NCBI homepage. The phylogenetic analysis was based on alignments of psoralen synthase (GenBank™ accession no. AAT06911.1) with translated CYP polypeptide sequences most related to psoralen synthase, which were either of undefined classification from *Citrus* (P450, AAL24049.1) or classified to CYP71 subfamilies from soybean (71A9, O81970.1; 71A10, AAB94584.1; 71D8, O81974.1; 71D9, O81971.1; 71D10, O48923.1), *Solanum melongena* (71A2, CAA50645.1; 71A4, CAA50312.1) and *Nepeta racemosa* (71A5, CAA70575.1; 71A6, CAA70576.1). None of these sequences has been functionally assigned. Menthofuran synthase from *Mentha piperita* (accession no. AF346833) was included as the only designated sequence. Furanocoumarins have been reported from *Citrus* sp., whereas soybean, *Solanum* and the Lamiaceae (*Nepeta* and *Mentha*) may accumulate simple coumarins. The sequences were aligned with multalign (Unitary Matrix), and phylogenetic analyses were carried out using ClustalW by the neighbor joining (NJ) method. The distances (percent divergence) between all pairs of sequences were calculated from multiple alignments, and the NJ method was applied to the distance matrix.

RESULTS

cDNA Cloning—The onset of furanocoumarin accumulation and the induction pattern of relevant enzyme activities in *A. majus* cell suspensions upon elicitor treatment was recorded previously (35–37, 39, 48) and suggested a period of 2–6 h of elicitation to be sufficient for maximal induction of transcript abundance. Total RNA was therefore isolated from cells treated for 3–5 h with fungal elicitor and employed as template for differential display RT-PCR amplifications of CYP-related ESTs. A stringent selection was achieved by an RT-PCR strategy of two rounds. The initial amplifications used combinations of an anchor primer and four forward primers deduced from the PERF motif (47), which was followed by a second round of nested PCR employing combinations of the anchor primer with eight decamer primers deduced from the conserved PFG motif (46). Distinct bands of 250–500 bp on agarose gel separation were reproducibly generated representing five divergent ESTs, which were extended to the full-size cDNAs by 3′- and 5′-RACE techniques. The cDNAs were sequenced and grouped (56) to CYP families 71 (accession no. AY532370.2), 73 (AY219918), 76 (AY532372.1), 82 (AY532373.1), and 98 (AY532371.2). *CYP73A41* was identified before to encode cinnamate 4-hydroxylase (48), and this report focused on *CYP71AJ1*, composed of a 1482-bp ORF flanked by 21 and 311

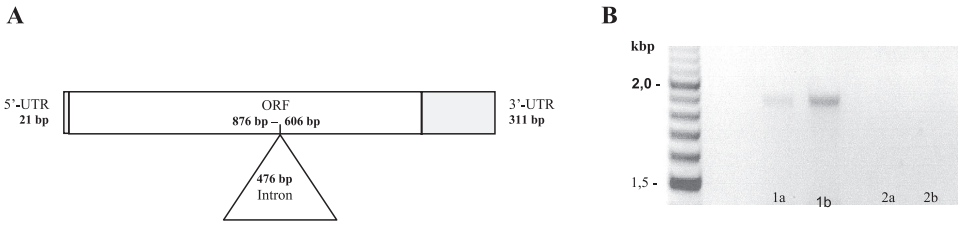

C

```
CYP73A1 1  MDLLLIEKTLVALFAAIIGAILISKLRGKKFKL
33
CYP71AJ1  1  MKMLEQNPQYLYFFSLFLVTIFLYKWLTLKKTPLKNLPPSPPQYPIIGNLHQIGPDPQAS   60
         61  LRDLAQKYGPLMFLKFGTVPVLVVSSADAAREALKTHDLVFADRPYSSVANKIFYNGKDM  120
        121  VFARYTEYWRQVKSICVTQLLSNKRVNSFHYVREEEVDLLVQNLENSHSKVANLTELLIE  180
        181  VTGNVVCRVSVGSGDKVDSYKILILEIMDMLGYSRSIEDFFPLLGWVDWLTGLRGKVAEA  240
        241  AKGVDTFLEGVLKEHLSTTGSKYNDFVSILLEIQEADAGSSMDNECIKSLIWDMLGAGTE  300
        301  TISTALEWTLAALIKNPDAMFKLQNEVREIGKGKSKISEADLVKMNYLQAVMKESMRLYF  360
        361  TAPLLVPREARODIKFMGYDISSGTQVLINAWAIARDPLLWDKPEEFRPERFLNSPIDYK  420
        421  GFHYEFLPFGAGRRGCPGIQFAMCINELVVANLVHKFNFELPDGKRLEDLDMTAASGITL  480
        481  RKKSPLLVVARPHV                                               494
```

FIGURE 2. *A*, schematic composition of *CYP71AJ1* containing a single intron. *B*, semiquantitative RT-PCR of *CYP71AJ1* employing end-to-end primers and total RNA as template from *A. majus* cells elicited for 3 (*lane 1a*) or 4 h (*lane 1b*) in comparison to RNA from control cells treated with water for 3 or 4 h (*lanes 2a* and *2b*). Molecular size markers are shown in the *left margin*. *C*, polypeptide sequences of *CYP73A1* (N terminus) and *CYP71AJ1* (full-size). Swapping of the boxed domains generated *CYP71AJ1mut*. The proline-rich region is *underlined*, the I-helix stretch *bold-printed*, and the conserved Cyt450 motifs (PERF and PFG to delineate primers) are *shaded*.

bp 5′- and 3′-UTRs, respectively (Fig. 2*A*). The inducibility of the selected transcript was initially verified by semiquantitative RT-PCR employing specific end-to-end oligonucleotide primers (Fig. 2*B*). The ORF encoded a polypeptide of 494 residues amounting to a calculated mass of 55891.15 Da with pI 6.49 (Fig. 2*C*). Software analysis predicted an *N*-terminal membrane insertion region and assigned the closest sequence relationship (66% similarity at most) to a few functionally undefined CYPs71, *e.g.* from *N. racemosa* (CYP71A5 and CYP71A6), *S. melongena* (CAA50312.1; CAA50645.1) or *A. thaliana* (CYP71A1), and to (+)-menthofuran synthase from peppermint (AF346833) (57). None of these plants has been reported to produce furanocoumarins. The relationship with menthofuran synthase (45% identity and 65% similarity) was nevertheless too low to assign a function to the polypeptide, and menthofuran has never been reported as a metabolite from *A. majus*. The authenticity of the cDNA was corroborated by cloning of the gene of 1961 bp, which revealed a single intron of 476 bp inserted at position 876 (Fig. 2*A*). Complementary Southern blotting suggested the presence of a small gene family of at least three copies in the *A. majus* genome (data not shown).

Functional Expression—Expression of CYP71AJ1 in yeast strains WAT11, WR, WAT21 under various regimes of culture conditions and induction temperature or in *E. coli* failed as monitored by enzyme assays with crude extracts, isolated microsomes, and CO difference spectroscopy (58). This was ascribed partly to the *in vitro* lability of *A. majus* coumarin-committed CYPs noted previously, presumably resulting from insufficient membrane association, or to low translational efficiency caused by an unfavorable codon bias on yeast expression of the *Ammi CYP71AJ1* sequence (59). Functional expression of CYPs in yeast cells may critically depend on the quality of the N-terminal anchor sequence as exemplified by CYP73A1 (cinnamate 4-hydroxylase) from *Helianthus tuberosus* (60). This enzyme was expressed with high activity in yeast WAT11 strain, and its N-terminal sequence was employed to enable or increase the expression of CYP73A17 and CYP73A15 in yeast microsomes (59, 61). Obviously, the modification of the anchor sequence does not modify the catalytic properties of CYPs (62, 63). Therefore, the N-terminal 37 amino acid residues of *CYP71AJ1* preceeding the proline-rich region and spanning the transmembrane helix residues 12–29 were replaced by the corresponding 33-residue membrane anchor region of *CYP73A1* (Fig. 2*C*).

Swapping of this domain generated *CYP71AJ1mut* which was expressed in yeast strain WAT11, grown for 24 h at 28 °C and induced for 18 h at 20 °C. Under these conditions, low level CYP expression (10.0 pmol/mg) was observed in microsomal fractions. Incubation of the isolated microsomes with (+)-pulegone, however, failed to yield menthofuran or any other product, and further incubations were conducted with demethylsuberosin, marmesin or psoralen as potential substrates. A product was observed from marmesin only (Fig. 3*A*), which required NADPH as a reductant (Fig. 3*B*) and was lacking in control incubations with microsomes from non-transformed yeast cells (Fig. 3*C*). Absorption spectra (λ_{max} 291 nm, broad shoulder at 329 nm) and mass spectra (Fig. 4) showing an M^+ of 186 as base peak with major fragments at m/z 158, 130, and 102 (loss of CO) unequivocally identified this product as psoralen. Thus, *CYP71AJ1mut* encoded psoralen synthase which is the first furanocoumarin-committed monooxygenase characterized at the molecular level after the cloning of bergaptol *O*-methyltransferase had been accomplished recently also from *A. majus* (39). Maximal psoralen synthase activity was observed in sodium phosphate buffer, pH 7.0 and at a temperature ranging from 27 to 35 °C.

Microsomes harvested from *CYP71AJ1mut* yeast transformants were also unstable upon storage and lost almost all psoralen synthase activity within 1 week at −80 °C. The advanced knowledge of assay and handling parameters prompted another approach to transform yeast cells with wild-type *CYP71AJ1*, which however failed to yield microsomes showing psoralen synthase activity. Nevertheless, yeast *CYP71AJ1* transformants were employed for precursor feeding studies, and a significant proportion of marmesin added to these cultures (1.0 mM) was converted to psoralen during an incubation period of 4 h, whereas yeast cells harboring the empty vector were inactive in this regard (Fig. 5). Overall, the data demonstrated that *CYP71AJ1* encodes psoralen synthase, which is probably too labile for detection in isolated yeast microsomes, in accordance

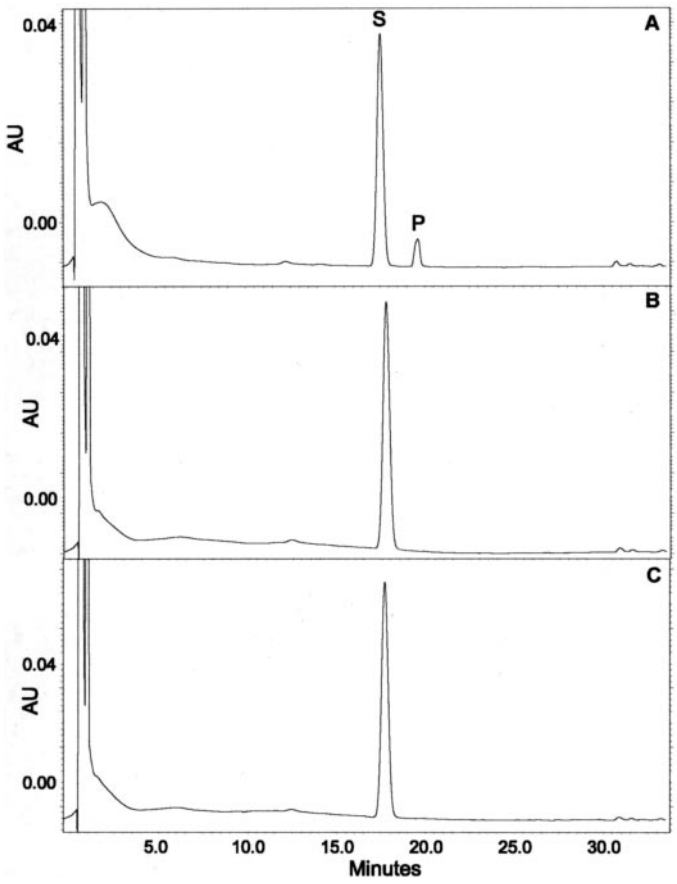

FIGURE 3. **HPLC separation profile of enzyme assays recorded at 300 nm.** The incubations were conducted in 0.1 M sodium phosphate buffer, pH 7.0, with 200.0 μM (+)-marmesin employing: *A*, microsomes from yeast CYP71AJ1*mut* transformants in the presence of 1.0 mM NADPH. *B*, microsomes as in *A* but without NADPH. *C*, microsomes from yeast transformed with the empty vector pYeDP60. *S*, (+)-marmesin (substrate); *P*, product.

with previous observations on *A. majus* microsomes (36, 42). The activity might be stabilized by adjustment of the N-terminal anchor sequence.

Cell cultures of *A. majus* accumulate various coumarins upon elicitation with bergapten as one major stable metabolite (12) and psoralen as an intermediate (Fig. 1). Therefore, the transient accumulation of psoralen, determined spectroscopically after HPLC separation, was correlated with the relative *CYP71AJ1* transcript abundance (Fig. 6). The ephemeral transcript abundance reached a sharp maximum at 4 h of elicitation followed by the maximal psoralen amount at 9–10 h. The induction patterns fully supported the functional significance of the *CYP71AJ1* transcript. Moreover, the negligible transcript abundance below 1 h of elicitation emphasized the previously proposed lack of background activity and *de novo* induction of this enzyme pivotal to psoralen synthesis (Fig. 6).

Substrate Specificity and Kinetic Analysis—A number of coumarins, furanocoumarins, phenylpropanoids, and two herbicides were examined under standard CYP assay conditions, but none except marmesin and 5-hydroxymarmesin served as a substrate (Table 1). The affinity of (+)-marmesin to the recombinant psoralen synthase determined at an apparent K_m of 1.5 ± 0.5 μM and k_{cat} 340 ± 24 min^{-1} is within range (46, 64) or exceeds (65) the substrate affinities of other enzymes of the CYP71 subfamily involved in plant secondary metabolism. 5-Hydroxymarmesin was also converted to bergaptol but with much lower affinity (K_m of 29.3 ± 8.0 μM) and specific activity (k_{cat} 143 ± 25 min^{-1}). No product, however, was formed from (+)-columbianetin, the angular analogue of (+)-marmesin (Fig. 1). Further examination revealed significant, albeit weak, inhibition of psoralen synthase activity by (+)-columbianetin (K_i of 225.0 μM), and this effect was competitive with the (+)-marmesin concentration (Fig. 7). Binding of (+)-marmesin and (+)-columbianetin at the same active site may suggest that only minor differences in the SRS topology distinguish psoralen and angelicin synthases. Various psoralens were reported to act as potent inhibitors of CYP activities by way of mechanism-based inhibition (66, 67). Accordingly, kinetic assays were conducted also in the presence of psoralen or 5- and 8-methoxypsoralen as well as angelicin. All of these compounds, however, failed to inhibit psoralen synthase *in vitro*, and this is consistent with the proposed evolutionary context suggesting that CYPs from furanocoumarin-producing plants, *i. e.* CYPs73A (C4Hs), are resistant to mechanism-based inhibition (48, 67). Furthermore, the lack of inhibition of psoralen synthase by angelicin is a prerequisite to support its suggested role as an inhibitor of psoralen detoxification by herbivores.

Modeling of the CYP71AJ1 Catalytic Site—Alignments with sequences of crystallized P450s (P450 BM3, CYP2C9, C8, C5, A6, and B4) were used to derive a comparative model for *A. majus* CYP71AJ1. Although the accuracy depends critically on the percentage sequence identity (CYP71AJ1 displays 27.5% similarity with CYP2C8) it is possible to build a reliable three-dimensional model based on the structural cores and several loop/helix regions that are highly conserved among the CYP families (55, 68–70). This model provided the basis for molecular docking of (+)-marmesin or (+)-columbianetin to predict the binding mode and to assign the SRS sequences (71, 72). Furthermore, the abstraction of hydrogen from C-3′ of (+)-marmesin in *syn*-configuration to the isopropyloxy side chain initiated by psoralen synthase (Fig. 1) (42, 43) requires the dihydrofuran moiety in juxtaposition above the iron of the heme moiety. Accordingly, the highest ranked docked solution fitted (+)-marmesin into a 45° angle aligned to the I helix (Ala^{297} to Ser^{303}; Fig. 2*C*) assigned to SRS4, with the dihydrofuran-ring proximal to residues Ala^{297} and Thr^{301} (Fig. 8*A*). Under these premises, the spatial distance of the *syn*-hydrogen at C-3′ of (+)-marmesin to the oxygen atom of the reactive iron-oxo heme approaches 3.78 Å, which likely supports psoralen synthase catalysis. The model enzyme-substrate complex revealed some commonality with CYP proteins such as insect CYP6B8 (21) placing Arg^{104} of SRS1 close to the heme carboxyl groups, probably stabilizing the ring in cooperation with Arg^{434} in the P450 signature motif, and lining the active site cavity above and below the coumarin ring system with hydrophobic residues Ala^{362}, Leu^{365}, Val^{366}, Pro^{367} of SRS5 and Val^{121}, Met^{120} of SRS1, respectively. However, hydrophilic residues Thr^{361} (SRS5) and Thr^{479} (SRS6) were assigned besides Thr^{301} (SRS4) to surround the dihydrofuran ring with isopropyloxy side chain in the catalytic pocket (Fig. 8*A*). In addition, Thr^{301} aligns with the conserved Thr of the P450 signature ((Ala/Gly)-Gly-*X*-

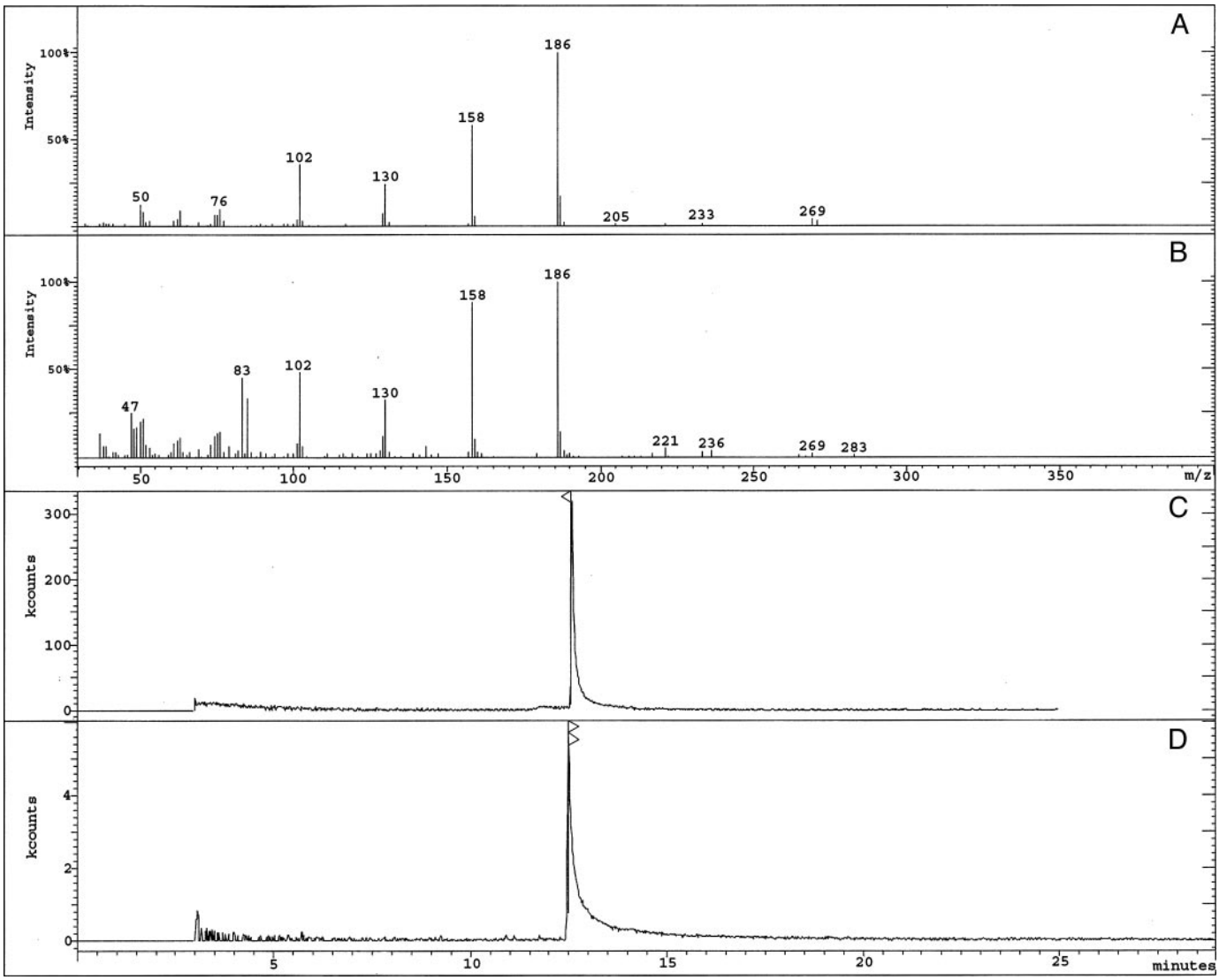

FIGURE 4. MS fragmentation (*A*) and GC separation profile (*C*) of the product isolated by incubation of (+)-marmesin with microsomes from yeast *CYP71AJ1mut* transformants in the presence of NADPH. The fragmentation pattern (*B*) and GC profile (*D*) of authentic psoralen were recorded for comparison.

(Asp/Glu)-Thr-(Thr/Ser) that is involved in dioxygen activation (74). The position of Thr^{301} near the active oxygen of the iron-oxo heme supports this role in CYP71AJ1. The analogous docked solution for (+)-columbianetin (Figs. 1 and 8*B*) suggested binding at the same topological site, which is compatible with competitive inhibition (Fig. 7), but revealed a distance of at least 6.27 Å between the 3′-*syn*-hydrogen and the iron-oxo center, which appears to exclude catalytic turnover.

Psoralen synthase described in this report is the only published monooxygenases sequence committed to furanocoumarin biosynthesis, and alignments are thus limited to less related sequences of mostly undefined functionality. Several monooxygenases degrading furanocoumarins were described from insects, and point mutations in their SRS1 region were reported to affect binding (10). These enzymes, however, share very little sequence homology with CYP71AJ1. Phylogenetic analysis (data not shown) revealed some relationship with a P450 from *Citrus sinensis* (62% similarity) or several members of the CYP71 family from *Solanum* melongena (A2 and A4; 64–65% similarity) and soybean (Ala^{9}, Ala^{10}, Asp^{8}, Asp^{9}, and Asp^{10}; 58–65% similarity) without functional assignment; these plants produce furanocoumarins (*Citrus*) or simple coumarins at least (*Solanum*, soybean). An equivalent level of similarity can be ascribed to functionally undefined CYP71A5 (68%) and CYP71A6 (65%) from *N. racemosa* or menthofuran synthase (65%) from *M. piperita*. Taking into account that the substrate-docked model assigned some residues of SRS1 and SRS5, in particular, to the active site, these sequence motifs were compared with the corresponding regions of CYPs from coumarin-producing plants (Table 2). The most peculiar features of psoralen synthase are residues Thr^{361} (SRS5) and Met^{120} (SRS1). While Met^{120} substitutes for hydrophobic Ile or Val in other CYP71 (Table 2), Thr^{361} in the YFT motif of CYP71AJ1 aligns with the HPP triplet conserved in almost all sequences of the CYP71 family. Replacement of both proline residues must considerably affect the spatial configuration of psoralen synthase and is conceivably involved in positioning Thr^{361} in the hydrophilic cluster about the isopropyloxy group of (+)-marmesin.

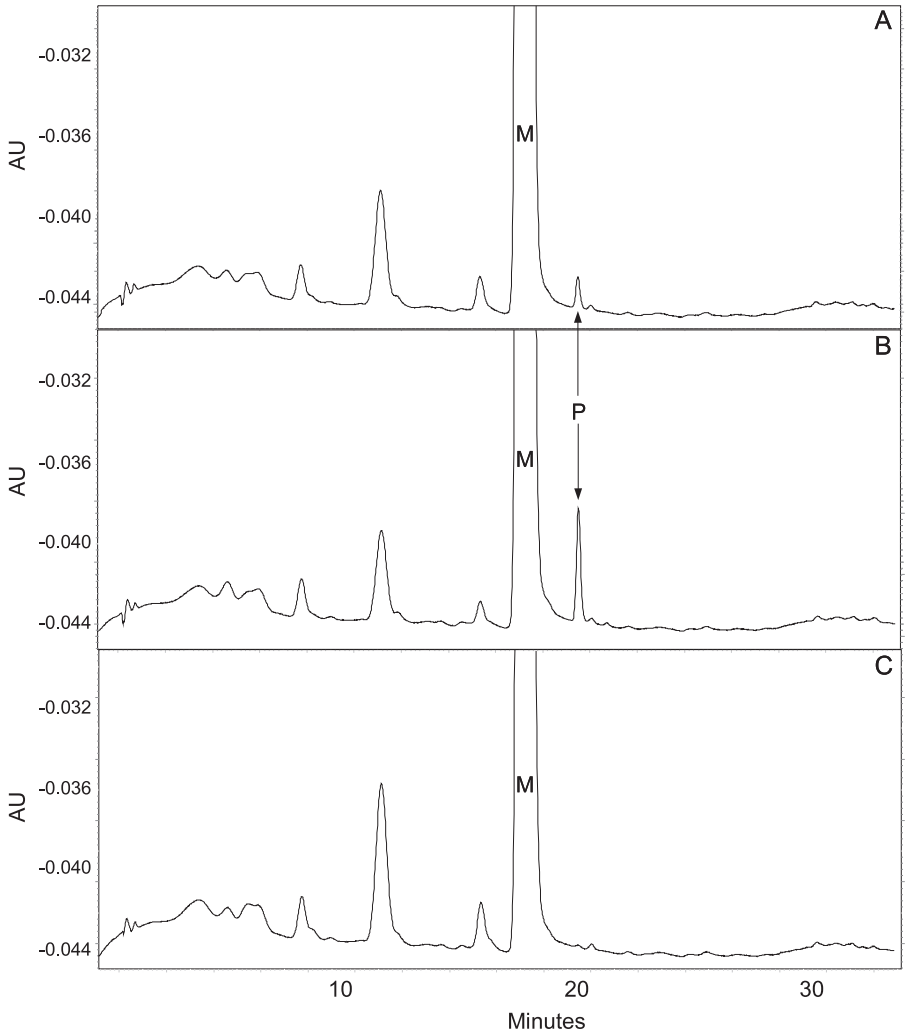

FIGURE 5. **Bioconversion of (+)-marmesin to psoralen in yeast culture.** Yeast cells transformed with *CYP71AJ1* (*A*), *CYP71AJ1mut* (*B*), or the empty vector (*C*) were grown in YPGE medium and induced by the addition of galactose for P450 expression. (+)-Marmesin was added to a final concentration of 1.0 mM, and the cells were incubated for an additional 4 h at 24 °C. The composition of the culture fluid was analyzed subsequently by HPLC at 300 nm. *M*, (+)-marmesin (substrate); *P*, Psoralen (product).

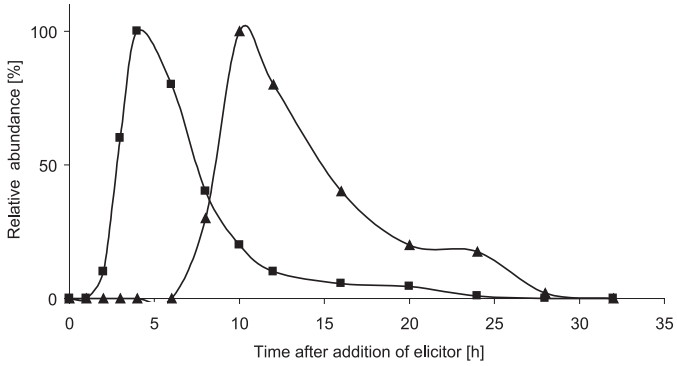

FIGURE 6. **Induction of *CYP71AJ1*transcript abundance (■) and transient amounts of psoralen (▲) in *A. majus* cell cultures following the addition of fungal elicitor.**

Site-directed Mutagenesis—To investigate the potential contributions of the depicted residues to the catalytic activity, Met^{120} was replaced by Val as the first step. The mutant was less readily expressed in yeast cells than the wild-type enzyme, but revealed also specificity for (+)-marmesin and did not accept (+)-columbianetin. Psoralen was the only product observed, and a K_m of 2.3 μM ± 0.39 μM was recorded for (+)-marmesin. This value is in range with the substrate affinity of the wild-type enzyme and suggests marginal effects of the M120V mutation, if any, on the catalytic activity.

DISCUSSION

Coumarins and furanocoumarins have been reported from numerous plants and their potential bioactivities have been recognized. Nevertheless, the biosynthesis of the 1-benzopyran-2-one nucleus and the molecular details of subsequent steps have remained incompletely understood (76). Three consecutive cytochrome P450-dependent reactions converting demethylsuberosin to bergaptol (Fig. 1) and identified in *Ammi* microsomes (35, 36) provided the basis for the differential cloning approach, which fully confirmed the previous proposal of separate CYP entities (31, 35, 36). Psoralen synthase represents the first cloned coumarin-committed monooxygenase, and CYP71AJ1 gives access to a new CYP71 subfamily of enzymes. Functional expression suffered from the instability and/or rather low specific activity of microsomes. This again confirmed our previous findings with microsomes from elicited *A. majus* cells which demanded unusually subtle conditions of cell propagation and fractionation, and the activity was lost rapidly even on storage of microsomes at −70 °C. It is conceivable that psoralen synthase activity essentially requires the tight association with the membrane and the reductase, which is supported by the beneficial effect of replacing the membrane insertion region by that of CYP73A1, although the activity of isolated microsomes remained unstable upon storage. Recombinant psoralen synthase showed narrow specificity and high affinity (K_m 1.5 μM) for (+)-marmesin (Table 1), compatible with the observation of (+)-marmesin as an intermediate of psoralen and bergaptol synthesis in elicited *A. majus* cells (36). An alternate pathway to bergaptol, however, appeared possible based on 5-hydroxylation of (+)-marmesin and subsequent cyclization. Recombinant psoralen synthase accepted 5-hydroxymarmesin (Table 1), and 5-hydroxymarmesin was included in an unconfirmed list of *A. majus* constituents (77). However, none of the original reports on *A. majus* coumarins (37, 75, 78–80) mentioned this compound, and psoralen syn-

TABLE 1
Compounds included in psoralen synthase substrate assays

Classification	Compound	R_t	l_{max}	K_m	k_{cat}
		min	*nm*	*μM*	min^{-1}
Substrate					
	(+)-Marmesin	19.0	334	1.5 ± 0.5	340.0 ± 24.0
	5-Hydroxymarmesin	18.0	339	29.3 ± 8.0	143.0 ± 35.0
No substrate					
Simple coumarins					
	Coumarin	12.3	280		
	Herniarin	14.3	323		
	Scopoletin	10.5	346		
	Umbelliferone	10.5	324		
	Demethylsuberosin	28.9	334		
Furanocoumarins					
	Psoralen	20.4	312		
	Bergaptol	14.2	314		
	Bergapten	17.5	312		
	Xanthotoxol	16.9	308		
	Xanthotoxin	15.6	302		
	Isopimpinellin	17.7	315		
	(+)-3,4,2′,3′-D_4-Columbianetin	19.8	328		
	Angelicin	21.4	302		
Cinnamic acids					
	Cinnamic acid	20.4	278		
	4-Coumaric acid	14.1	310		
	2-Coumaric acid	13.0	283		
	Ferulic acid	12.7	315		
Monoterpenes					
	(+)-Pulegone	21.5	258		
	Menthofuran	22.0	288		
Herbicides					
	Isoproturon	23.0	238		
	Chlortoluron	22.0	283		

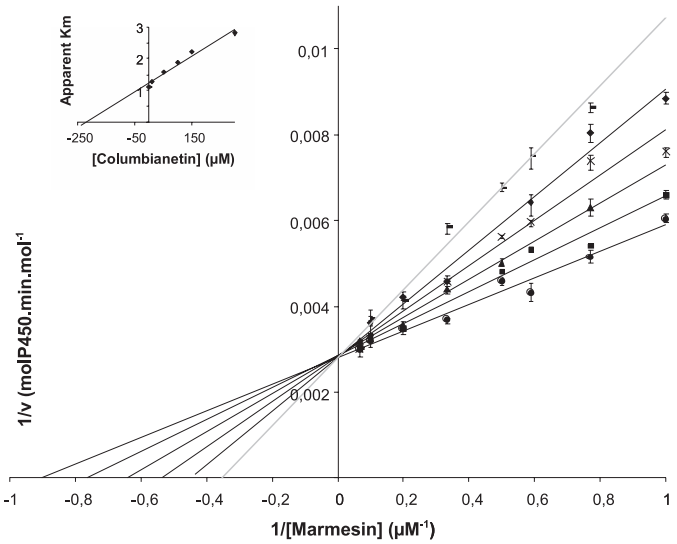

FIGURE 7. **Competitive inhibition of psoralen synthase (CYP71AJ1mut) activity by (+)-columbianetin.** The assays were conducted in the absence (●) and in the presence of (+)-columbianetin fixed at 10.0 (■), 50.0 (▲), 100.0 μM (×), 150 μM (◆), and 300 μM (■) concentration. The apparent K_m values inferred from the Lineweaver-Burk diagram plotted *versus* the concentration of (+)-columbianetin (*inset*) revealed an apparent K_i of about 225.0 μM. Data are means of triplicate experiments.

thase was shown before to tolerate *in vitro* minor changes of substrate, such as the linear 2′-acetyl-dihydrofuranocoumarin (43). This likely excludes the alternate route to bergaptol in *A. majus* and is corroborated by the data presented in this report. The low conversion rate of 5-hydroxymarmesin (k_{cat}/K_m 4.9) as compared with (+)-marmesin (k_{cat}/K_m 226) assigned 5-hydroxymarmesin as an inefficient substrate for CYP71AJ1 and unlikely precursor for bergaptol in *A. majus*.

On the assumption that the capacity for angular furanocoumarin formation has evolved from the linear furanocoumarin pathway, related or highly homologous enzymes should be expected to catalyze the analogous reactions in both pathways. The oxidative chain cleavage reactions of (+)-marmesin and (+)-columbianetin (Fig. 1) appear highly analogous, and *syn*-elimination has been confirmed also for the conversion of (+)-columbianetin to angelicin (34) suggesting a cytochrome P450-dependent mechanism. Moreover, the competitive inhibition kinetics documented in this report indicate that (+)-columbianetin binds to the active site of psoralen synthase, but fails to serve as a substrate. Fitting of (+)-columbianetin into the active site of the CYP71AJ1 model may explain this discrepancy, because the highest ranked docked solution placed the *syn*-configurated hydrogen at carbon-3′ 6.27 Å away from the iron-oxo center (Fig. 8*B*), which is much less favorable than the 3.78 Å calculated in the case of (+)-marmesin (Fig. 8*A*). Although the data are not yet sufficient to draw conclusions on the evolution of the pathway to angular furanocoumarins, it is tempting to assume that a limited number of mutations may have transformed psoralen synthase to angelicin synthase, concerning primarily Thr^{301}, Thr^{361}, and the residues Ala^{362}, Leu^{365}, and Val^{366} in the active site cavity (Fig. 8, *A* and *B*). Nevertheless, another major branchpoint in linear *versus* angular furanocoumarin formation exists at the stage of prenylation of umbelliferone (Fig. 1). Prenylation reactions at C-6 and O-7, but no C-8-prenylation, of umbelliferone were observed in *A. majus* (37), and thus more than one hurdle must be overcome to enter the route to angular furanocoumarins. These aspects cannot be studied in *A. majus* because of lack of angular furanocoumarins, but might be conducted in

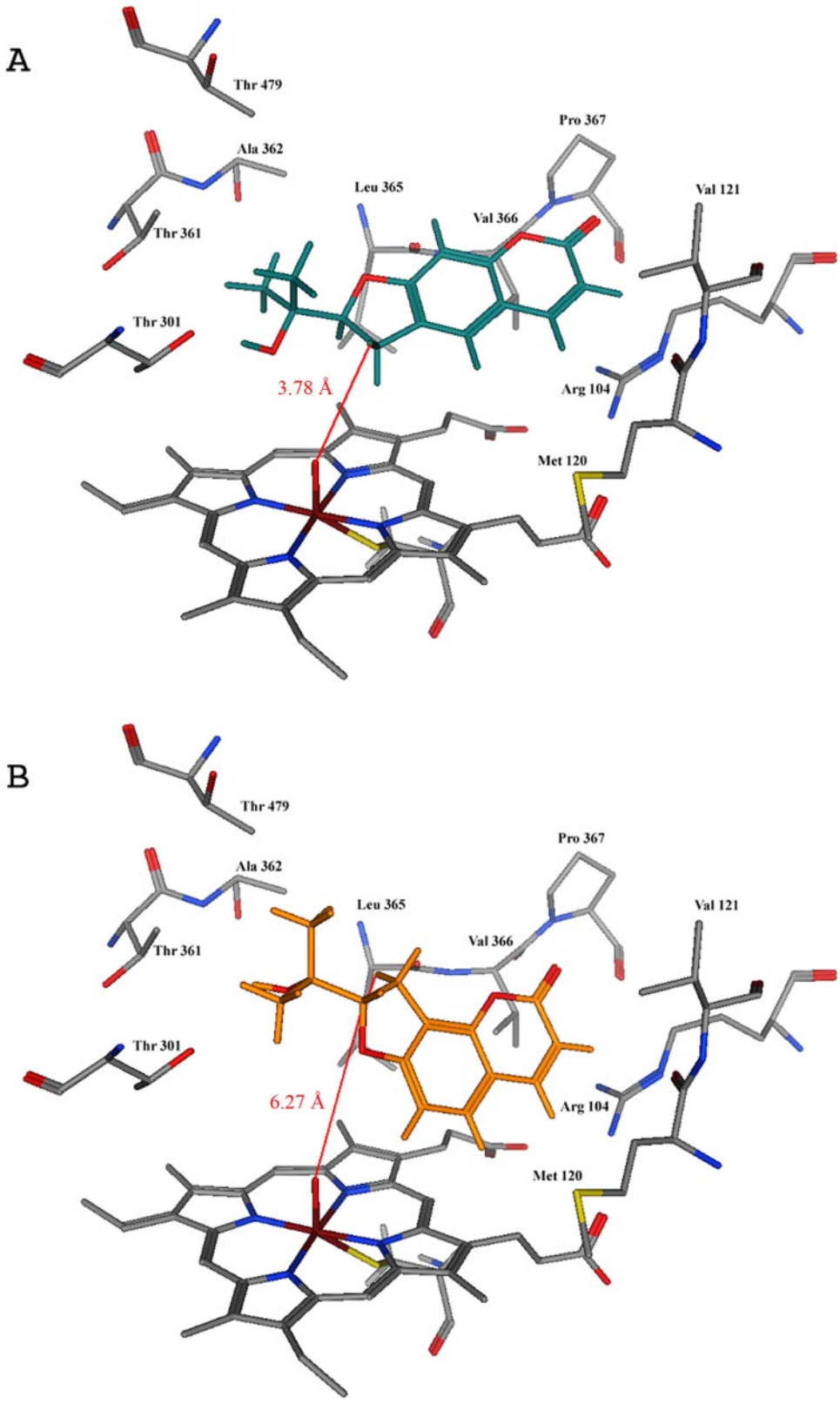

FIGURE 8. **Docking of (+)-marmesin (*A*) or (+)-columbianetin (*B*) into the active site of the CYP71AJ1 three-dimensional model.** Amino acid residues lining the active site and the heme in the iron-oxo state are designated and presented in *gray* with *red oxygen* and *blue nitrogen* atoms. The best ranked docking mode for (+)-marmesin (*A*; depicted in *green*) places the C3′-*syn*-hydrogen 3.78 Å proximal to the oxygen of the reactive iron-oxo heme, whereas the corresponding C3′-hydrogen of (+)-columbianetin (*B*; shown in *orange*) is assigned more distant (6.27 Å) from the iron-oxo heme.

Heracleum or *Angelica* species (1, 43). The capacity to produce the angular set of furanocoumarins has been proposed to evolve late and as an ecotoxicological consequence of psoralen detoxification (30). The fact that angular furanocoumarins always accumulate concomitantly with linear furanocoumarins might offer a chance to isolate a hybrid psoralen/angelicin synthase from these plants as a firm proof of the evolutionary context.

The SRS have been defined as regions relevant for substrate specificity (71), and common sequence motifs might be expected in CYPs accepting structurally related substrates. Psoralen synthase, however, is the first monooxygenase cloned from the furanocoumarin pathway and catalyzes a reaction without precedent in the literature. Provisional partial alignments of SRSs revealed significant differences to sequentially related, but functionally unassigned, CYPs only in the Tyr^{359}-Phe-Thr triplet (SRS5) and Met^{120} residue (SRS1). Whereas Met is of intermediate polarity and replaces Ile or Val, the triplet aligns to His-Pro-Pro in other CYPs (Table 2) and conceivably causes significant changes in substrate binding and/or reactivity. Based on the initial site-directed mutagenesis replacing Met^{120} by Val, this residue appears to be of minor significance. However, the residues of the triplet in SRS5 are likely to affect the overall enzyme structure and remain to be replaced aiming at the modulation of substrate specificity. Furthermore, the SRS5 sequence might provide a basis for cloning of those CYPs acting consecutively with psoralen synthase in the furanocoumarin pathway, *i. e.* marmesin synthase or psoralen 5- and 8-monooxgenases. Psoralen synthase was identified as a member of the CYP71 family, which is the largest plant CYP family and contains numerous duplicated genes (74). It appears possible that the monooxygenases of the furanocoumarin pathway evolved from one ancestor gene as was dem-

TABLE 2
Alignment of partial recognition sites

SRS1 (Arg^{104}–Val^{121})				
Psoralen synthase	RPYSS	VANKI	FYNGK	DMV
P450 Citrus sinensis	RPPLI	GSGKF	TYNYS	DIA
CYP71A9	RPSLY	AANRL	GYG-S	TVS
CYP71A10	RRQPT	AAKIF	GYGCK	DVA
CYP71D8	RPQLL	APQFM	VYGAT	DIA
CYP71D9	RPYVL	AAEIM	DYDFK	GVA
CYP71D10	RPDFV	LSRIV	SYNGS	GIV
SRS5 (Leu^{358}–Glu^{369})				
Psoralen synthase	LYFTA	PLLVP	RE	
P450 Citrus sinensis	LHPPA	PLLIA	RD	
CYP71A9	LHPPA	PLLVP	RE	
CYP71A10	LHPPL	PLLIA	RE	
CYP71D8	LHPPS	QLI-P	RE	
CYP71D9	LHPPA	PLLLP	RE	
CYP71D10	LHPPV	PLLVP	RV	

onstrated for the CYPs catalyzing the DIMBOA/ DIBOA pathway in maize (73).

Acknowledgments—We thank Prof. G. Innocenti (Padova, Italy) for samples of (+)-marmesin and 5-hydroxymarmesin, Prof. W. Boland (Jena, Germany) for the gift of (+)-3,4,2′,3′-D_4-columbianetin, and Dr. S. Martens for valuable discussions.

REFERENCES

1. Murray, R. D. H., Méndez, J., and Brown, S. A. (1982) *The Natural Coumarins: Occurrence, Chemistry and Biochemistry*, Wiley, New York
2. Murray, R. D. (1991) *Progr. Chem. Org. Natural Prod.* **58,** 83–316
3. Estévez-Braun, A., and González, A. G. (1997) *Natural Product Rep.* 465–475
4. Wulff, H., Rauer, H., During, T., Hanselmann, C., Ruff, K., Wrisch, A., Grissmer, S., and Haensel, W. (1998) *J. Med. Chem.* **41,** 4542–4549
5. Kawase, M., Sakagami, H., Motohashi, N., Hauer, H., Chatterjee, S. S., Spengler, G., Vigyikanne, A. V., Molnar, A., and Molnar. J. (2005) *In Vivo* **19,** 705–711
6. Malaiyandi, V., Sellers, E. M., and Tyndale, R. F. (2005) *Clin. Pharmacol. Therap.* **77,** 145–158
7. De Castro, W. V., Mertens-Talcott, S., Rubner, A., Butterweck, V., and Derendorf, H. (2006) *J. Agric. Food Chem.* **54,** 249–255
8. Wen, Y. H., Sahi, J., Urda, E., Kulkarni, S., Rose, K., Zheng, X., Sinclair, J. F., Cai, H., Strom, S. C., and Kostrubsky, V. E. (2002) *Drug Metabolism* **30,** 977–984
9. Paine, M. F., Criss, A. B., and Watkins, P. B. (2005) *J. Pharmacol. Exp. Ther.* **312,** 1151–1160
10. Pan, L., Wen, Z., Baudry, J., Berenbaum, M. R., and Schuler, M. A. (2004) *Arch. Biochem. Biophys.* **422,** 31–41
11. Elgamal. M. H. A., Shalaby, N. M. M., Duddeck, H., and Hiegemann M. (1993) *Phytochemistry* **34,** 819–823
12. Hamerski, D., Beier, R. C., Kneusel, R. E., Matern, U., and Himmelspach, K. (1990) *Phytochemistry* **29,** 1137–1142
13. Ekiert, H., and Gomólka, E. (2000) *Pharmazie* **55,** 684–687
14. Tietjen, K. G., Hunkler, D., and Matern, U. (1983) *Eur. J. Biochem.* **131,** 401–407
15. Beier, R. C., Ivie, G. W., and Oertli, E. H. (1994) *Phytochemistry* **36,** 869–872
16. Innocenti, G., Cappelletti, E. M., and Caporale, G. (1986) *Plantes Médicinales et Phytothérapie* **4,** 313–322
17. Zobel, A. M., and Brown, S. A. (1990) *J. Chem. Ecol.* **16,** 1623–1634
18. Zobel, A. M., and Brown, S. A. (1991) *J. Chem. Ecol.* **17,** 1801–1810
19. Städler, E., and Roessingh, P. (1990) *Symp. Biol. Hung.* **39,** 71–85
20. Afek, U., Carmeli, S., and Aharoni, N. (1995) *Phytochemistry* **39,** 1347–1350
21. Li, X., Baudry, J., Berenbaum, M. R., and Schuler, M. A. (2004) *Proc. Natl. Acad. Sci. U. S. A.* **101,** 2939–2944
22. Kanne, D., Straub, K., Rapoport, H., and Hearst, J. E. (1982) *Biochemistry* **21,** 861–871
23. Gruenert, D. C., Ashwood-Smith, M., Mitchell, R. H., and Cleaver, J. E. (1985) *Cancer Res.* **45,** 5394–5398
24. Berenbaum, M. R., Nitao, J. K., and Zangerl, A. R. (1991) *J. Chem. Ecol.* **17,** 207–215
25. Berenbaum, M. R., and Zangerl, A. R. (1996) *Recent Adv. Phytochem.* **30,** 1–24
26. Ma, R., Cohen, M. B., Berenbaum, M. R., and Schuler, M. A. (1994) *Arch. Biochem. Biophys.* **310,** 332–340
27. Wen, Z., Pan, L., Berenbaum, M. R., and Schuler, M. A. (2003) *Insect. Biochem. Mol. Biol.* **33,** 937–947
28. Berenbaum, M. R., and Feeny, P. (1981) *Science* **212,** 927–929
29. Berenbaum, M. R., and Zangerl, A. R. (1993) *Oecologia* **95,** 370–375
30. Berenbaum, M. R., and Zangerl, A. R. (1998) *Proc. Natl. Acad. Sci. U. S. A.* **95,** 13743–13748
31. Matern, U., Lüer, P., and Kreusch, D. (1999) in *Comprehensive Natural Products Chemistry* (Sankawa, U., ed), Vol. 1, pp. 623–637. Elsevier, Amsterdam
32. Dhillon, D. S., and Brown, S. A. (1976) *Arch. Biochem. Biophys.* **177,** 74–83
33. Stanjek, V., Piel, J., and Boland, W. (1999) *Phytochemistry* **50,** 1141–1145
34. Stanjek, V., and Boland W. (1998) *Helv. Chim. Acta* **81,** 1596–1607
35. Hamerski, D., and Matern, U. (1988a) *FEBS Lett.* **239,** 263–265
36. Hamerski, D., and Matern, U. (1988b) *Eur. J. Biochem.* **171,** 369–375
37. Hamerski, D., Schmitt, D., and Matern, U. (1990) *Phytochemistry* **29,** 1131–1135
38. Wendorff, H., and Matern, U. (1986) *Eur. J. Biochem.* **161,** 391–398
39. Hehmann, M., Lukacin, R., Ekiert, H., and Matern, U. (2004) *Eur. J. Biochem.* **271,** 932–940
40. Boland, W., Gäbler, A., Gilbert, M., and Feng, Z. (1998) *Tetrahedron* **54,** 14725–14736
41. Lieberman, S., and Lin, Y. Y. (2001) *Steroid Biochem. Mol. Biol.* **78,** 1–14
42. Stanjek, V., Miksch, M., Lüer, P., Matern, U., and Boland, W. (1999) *Angew. Chemie-Int. Ed.* **38,** 400–402
43. Stanjek, V. (1998) *Studien zur Biosynthese der Furanocumarine.* PhD Thesis, Universität Bonn
44. Hagemeier, J., Batz, O., Schmidt, J., Wray, V., Hahlbrock, K., and Strack, D. (1999) *Phytochemistry* **51,** 629–635
45. Giuliano, G., Bartley, G. E., and Scolnik, P. A. (1993) *Plant Cell* **5,** 379–387
46. Schopfer, C. R., and Ebel, J. (1998) *Mol. Gen. Genet.* **258,** 315–322
47. Fischer, T. C., Klattig, J. T., and Gierl, A. (2001) *Theor. Appl. Genet.* **103,** 1014–1021
48. Hübner, S., Hehmann, M., Schreiner, S., Martens, S., Lukacin, R., and Matern, U. (2003) *Phytochemistry* **64,** 445–452
49. Dellaporta, S. J., Wood, J., and Hick, J. B. (1983) *Plant Mol. Biol. Rep.* **1,** 19–21
50. Pompon, D., Louerat, B., Bronne, A., and Urban, B. (1996) *Methods Enzymol.* **272,** 51–64
51. Gietz, D., St. Jean, A., Woods, R. A., and Schiestl, R. H. (1992). *Nucleic Acids Res.* **20,** 1425
52. Diesperger, H., and Sandermann, H., Jr. (1978) *FEBS Lett.* **85,** 333–336
53. Bradford, M. M. (1976) *Anal. Biochem.* **72,** 248–254
54. Omura, T., and Sato, R. (1964) *J. Biol. Chem.* **239,** 2370–2378
55. Baudry, J. Li, W., Pan, L., Berenbaum, M. R., and Schuler, M. A. (2003) *Protein Eng.* **16,** 577–587
56. Specker, S. (2004) *Klonierung von Cytochrom P450-abhängigen Monooxygenasen aus Ammi majus* L. und funktionelle Expression der Zimtsäure 4-Hydroxylase. PhD Thesis, Philipps-Universität, Marburg
57. Croteau, R. B., Davis, E. M., Ringer, K. L., and Wildung, M. R. (2005) *Naturwissenschaften* **92,** 562–577
58. Jefcoate, C. R. (1978) *Methods Enzymol.* **52,** 258–279
59. Batard, Y., Hehn A., Nedelkina, S., Schalk, M., Pallett, K., Schaller, H., and Werck-Reichhart, D. (2000) *Arch. Biochem. Biophys.* **379,** 161–169
60. Teutsch, H. G., Hasenfratz, M. P., Lesot, A., Stoltz, C., Garnier, J. M., Jeltsch, J. M., Durst, F., and Werck-Reichhart, D. (1993) *Proc. Natl. Acad. Sci. U. S. A.* **90,** 4102–4106

61. Nedelkina, S., Jupe, S. C., Blee, K. A., Schalk, M., Werck-Reichhart, D., and Bolwell, G. P. (1999) *Plant Mol. Biol.* **39,** 1079–1090
62. Richardson, T. H., Jung, F., Griffin, K. J., Wester, M., Raucy, J. D., Kemper, B., Bornheim, L. M., Hasset, C., Omiecinski, C. J., and Johnson, E. F. (1995) *Arch. Biochem. Biophys.* **323,** 87–96
63. Sueyoshi, T., Park, L. J., Moore, R., Juvonen, R. O., and Negishi, M. (1995) *Arch. Biochem. Biophys.* **332,** 265–271
64. Latunde-Dada, A. O., Cabello-Hurtado, F., Czittrich, N., Didierjean, L., Schopfer, C., Hertkorn, N., Werck-Reichhart, D., and Ebel, J. (2001) *J. Biol. Chem.* **276,** 1688–1695
65. Takahashi, S., Zhao, Y., O'Maille, P. E., Greenhagen, B. T., Noel, J. P., Coates, R. M., and Chappell, J. (2005) *J. Biol. Chem.* **280,** 3686–3696
66. Koenigs, I. L., and Trager, W. F. (1998) *Biochemistry* **37,** 13184–13193
67. Gravot, A., Larbat, R., Hehn, A., Lièvre, K., Gontier, E., Goergen, J-L., and Bourgaud, F. (2004) *Arch. Biochem. Biophys.* **422,** 71–80
68. Kemp, C. A., Maréchal, J-D., and Sutcliffe, M. J. (2005) *Arch. Biochem. Biophys.* **433,** 361–368
69. Williams, P. A., Cosme, J., Sridhar, V., Johnson, E. F., and McRee, D. E. (2000) *J. Inorg. Biochem.* **81,** 183–190
70. Rupasinghe, S., Baudry, J., and Schuler, M. A. (2003) *Protein Eng.* **16,** 721–731
71. Gotoh, O. (1992) *J. Biol. Chem.* **267,** 83–90
72. Werck-Reichhart, D., and Feyereisen, R. (2000) *Genome Biol.* **1,** 1–9
73. Frey, M., Huber, K., Park, W. J., Sicker, D., Lindberg, P., Meeley, R. B., Simmons, C. R., Yalpani, N., and Gierl, A. (2003) *Phytochemistry* **62,** 371–376
74. Werck-Reichhart, D., Bak, S., and Paquette, S. (2002) *The Arabidopsis Book*, pp. 1–28, The American Society of Plant Biologists, Rockville, MD
75. Herde A. (2005) *Untersuchung der Cumarinmuster in Früchten ausgewählter Apiaceae*, Ph.D. Thesis, Universität Hamburg
76. Bourgaud, F., Hehn, A. Y., Larbat, R., Doerper, S., Gontier, E., Kellner, S., and Matern, U. (2006) *Phytochem. Rev.* in press
77. Ur-Rahman, A., Said, H. M., and Ahmad, V. U. (1986) *Encyclopedia Planta Medica*, Vol. 1, p. 373, Hamdard Foundation Press, Karachi, Pakistan
78. Ivie, G. W. (1978) *J. Agric. Food Chem.* **26,** 1394–1402
79. Królicka, A., Staniszewska, I., Bielawski, K., Malinski, E., Szafranek, J., and Lojkowska, E. (2001) *Plant Sci.* **160,** 259–264
80. Pande, D., Purohit, M., and Srivastava, P. S. (2002) *Plant Sci.* **162,** 583–587